

## Study of mechanical and optical properties of MoSiN membranes

© O.V. Novikova, E.E. Gusev, A.A. Epikhin, I.V. Kushnarev, P.S. Ivanin, E.A. Lebedev, N.A. Dyuzhev

National Research University of Electronic Technology (MIET), 124498 Zelenograd, Moscow, Russia

E-mail: kamatjma@mail.ru

Received June 23, 2025

Revised August 14, 2025

Accepted August 14, 2025

A new correlation has been established between the structural (surface roughness and grain size), mechanical (mechanical strength, elastic modulus), and optical (absorption coefficient) properties of MoSiN at different annealing temperatures. Thin-film MoSiN layers were deposited by magnetron sputtering in a nitrogen-argon gas atmosphere. During the experiment, a circular MoSiN membrane structure was fabricated by group technology. Atomic force microscopy determined the roughness of the as-deposited film to be  $1.5 \pm 0.1$  nm. Using the ImageJ software and SEM images, the average grain size of the initial MoSiN was calculated as 22 nm. The Young's modulus of MoSiN was found to be 96 GPa. Using a mechanical testing setup, the critical pressure was measured as  $0.05 \pm 0.003$  GPa for 10 samples. The mechanical strength of the MoSiN structure was calculated as 1.15 GPa. The absorption coefficient exhibited only minor variation within the wavelength range of 400–900 nm. To study possible changes in the material properties during photolithography, a simulation of the process in the form of additional thermal treatment of MoSiN was carried out.

**Keywords:** mechanical strength, silicon molybdenum, membranes, thin films.

DOI: 10.61011/SC.2025.06.62058.7738

### 1. Introduction

When developing a coating material, it is necessary to make a choice between resistance to mechanical influences and optical properties [1]. One of the solutions is the use of multilayer coatings [2], in which the top layer can provide high transparency, and the bottom layer can provide scratch resistance. Another approach is additional surface treatment, such as ion stripping in argon plasma or oxygen [3]. Impurities are also added to the thin-film material through ion implantation to improve the optical or mechanical properties [4]. In addition, it is possible to change the structural properties of the composite material by changing the ratio between the concentration of atoms. It was shown in Ref. [5] that when the Si content in the MoSiN coating is  $> 12$  at.%, the structure of the material changes from the initially crystalline phase to the amorphous phase.

To increase the transmission coefficient, it is necessary to reduce the thickness of the material through which the radiation passes. However, films change their mechanical properties during the transition from macro- to micro- and nano-thicknesses [6]. Ignorance of the exact mechanical properties (mechanical strength, biaxial modulus of elasticity) prevents the developer from designing devices, in particular photomask coatings. In this research paper, molybdenum silicide films (with nitrogen addition) are considered, which are actively used as functional layers in photomasks (in the spectral range with a wavelength of  $\lambda = 193$ –248 nm) to shift the phase of the wave by

180° [7,8] and to protect the underlying layer from dust particles and deformations.

MoSiN coatings are of high importance due to their ultrahigh hardness, increased strength, wear resistance, corrosion and abrasion resistance [9], and thermal stability. The key characteristics for membrane films are their tensile strength and elastic properties. To assess the reliability of the finished product, it is necessary to know the mechanical strength of the components. For example, a film used as an absorption filter must maintain its mechanical integrity during various operations, such as transportation, installation in a vacuum chamber, pumping air and blowing gases. The grain size and surface roughness affect the wear resistance of the material and its optical components, such as reflection and scattering of light.

Also, in photolithographic installations, the process of exposure with an excimer ArF laser heats [10] the entire system, including a photomask with a functional MoSiN layer. Heating of the template can lead to changes in the structural and mechanical properties of the material, which directly affect the accuracy and quality of image transfer to the substrate. In this work, the analogue of laser exposure during photolithography is additional heat treatment in a thermocompression bonding unit for 1 hour to temperatures of 100, 200, 300 and 400 °C. The heating temperature may vary in the photolithography process using the MoSiN [11] protective coating depending on the specific process and the requirements for adhesion and curing. Typically, during the material curing process,

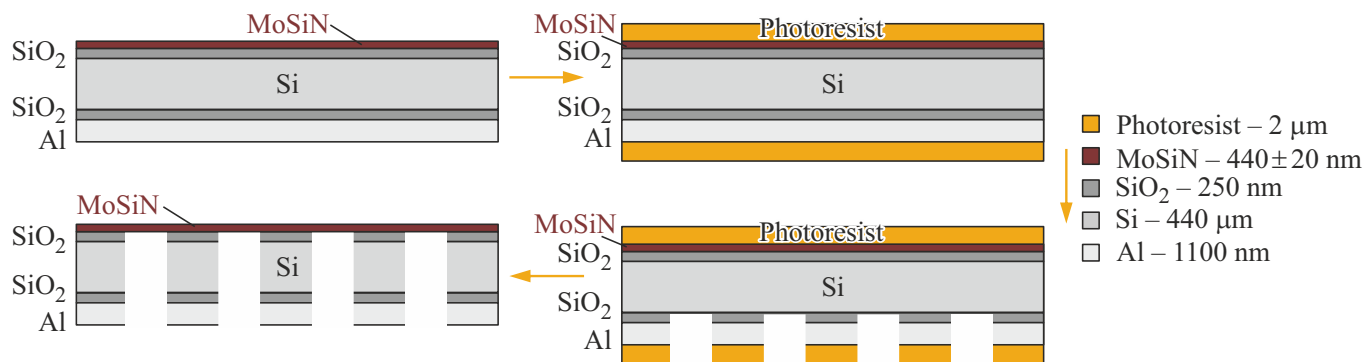


**Figure 1.** Technological route for manufacturing the MoSiN membrane structure.

the temperature can reach 150–200 °C to ensure optimal conditions for bonding and improved adhesion of the coating to the substrate. Usually, the duration of exposure to radiation when exposing a photomask with a laser does not exceed several minutes.

## 2. Structure manufacturing technology

During the experiment, a MoSiN membrane structure was manufactured, the manufacturing route of which is shown in Figure 1.

A plate made of monocrystalline KEF4.5 silicon with a diameter of 150 mm with a crystallographic orientation of (100) and a thickness of 400 μm was used. A layer of SiO<sub>2</sub> with a thickness of 250 nm each was initially applied on both sides of the plate. Silicon oxide performs the functions of a stop layer during deep anisotropic etching of a silicon wafer. An Al protective film with a thickness of 1100 nm was formed by magnetron sputtering. The MoSiN film was also formed by magnetron sputtering with a thickness of  $440 \pm 20$  nm (Figure 2).

Sputtering of MoSiN targets with 99.5 % purity thickness was performed in a medium of a mixture of argon and nitrogen. The flow of each of the gases was independently controlled. The functional purpose of nitrogen addition in the structure under study is to control phase shift and transmission (for DUV photolithography with wavelength  $\lambda = 193$ –248 nm). It should be noted that plasma activation of the surface was required before the liquid chemical etching of Al and two layers of SiO<sub>2</sub> to increase the etching rate in the liquid etcher. Silicon was locally removed by the Bosch process (in an SF<sub>6</sub>/C<sub>4</sub>F<sub>8</sub> medium) to the SiO<sub>2</sub> layer. As a result, a circular membrane with a diameter of  $160 \pm 20$  μm was formed on a square-shaped Si crystal with a side of 6 mm.

For additional heat treatment of the structure, a bonding chamber with a vacuum atmosphere of  $10^5$  Pa was used at a temperature range from 100 to 400 °C.

## 3. Analytical equipment

An automated pressure supply stand was used to determine the critical pressure. The automated stand includes: a main with the possibility of supplying air (vacuum, argon or other gas) with a pressure of up to 0.7 GPa; a cylinder receiver with an analog pressure gauge; filter regulator MC104-D00; proportional pressure regulator ER104-5PAP; Arduino Mega 2560 board; printed circuit board with various components; computer; Veeco Wyko NT9300 profiler; instrument table. The cylinder receiver acts as a surge tank to smooth the gas pressure drops, as well as for ensuring the overall stability of the system. The supplied air enters the filter regulator MC104-D00 with HDPE membrane type filter element with a filtration degree of 25 μm according to ISO 8573-1:2010. The pressure regulator is responsible for maintaining a constant and controlled level of overpressure. Several pressure gauges are located at various points of the test bench for ensuring real-time monitoring of pressure levels. There are also built-in safety valves for automatic relief of overpressure in case of rupture of the membrane. The software for the Arduino Mega 2560 board allows controlling the supply and pressure relief at the desired frequency. The accuracy of the overpressure supply is 0.001 atm. The accuracy of measuring the relief (deflection of the membrane) along the vertical axis was at least 5 nm on the Veeco Wyko NT9300 profiler.

The AIST SmartSPM-1000 atomic force microscope (AFM) was used to determine the roughness parameter. The measurements were carried out in a semi-contact (tapping) mode. High-resolution silicon AFM cantilevers of the NSG01 series were used, designed for semi-contact and contactless scanning modes. The guaranteed resonant frequency range was 70–110 kHz, the typical value of the force constant — 5.1 N/m. The cantilevers had an Al reflective coating.

A scanning electron microscope (SEM) and the ImageJ program were used to determine the average size of MoSiN grains. The Sentech SENresearch 4.0 spectroscopic ellipsometer was used to determine the optical properties.

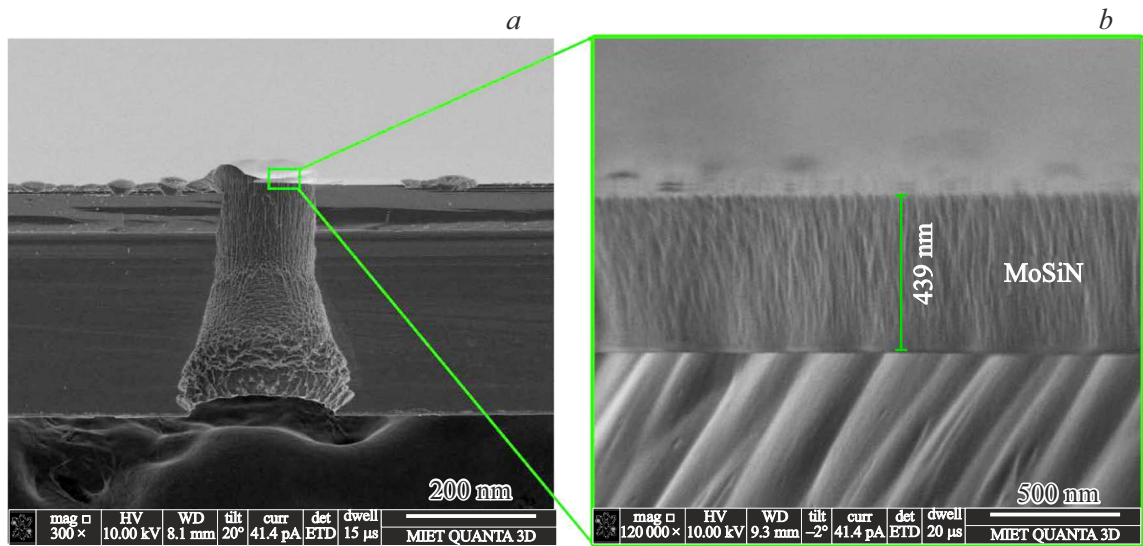


**Figure 2.** Membrane structure under study. The image was obtained using SEM.

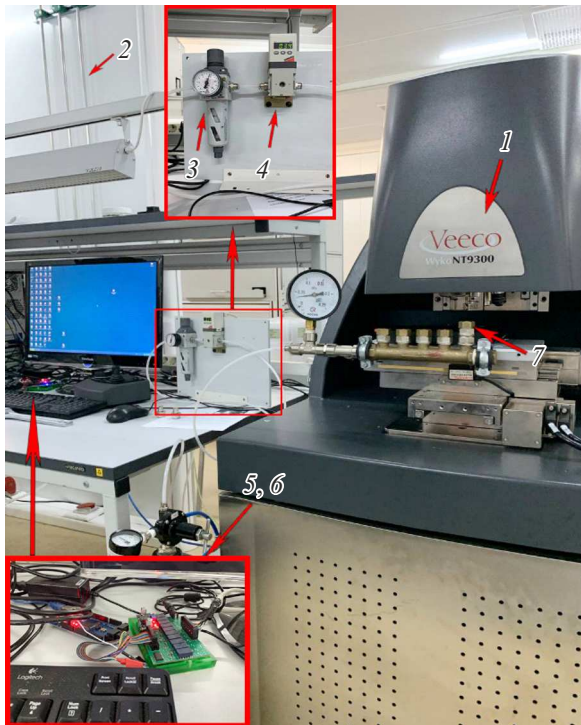


**Figure 3.** Stand for measuring the mechanical and structural properties of thin films: 1 — Veeco Wyko NT9300 optical profiler, 2 — main line, 3 — filter regulator, 4 — proportional regulator pressure, 5 — Arduino Mega 2560 board, 6 — printed circuit board with various components, 7 — sample.

#### 4. Analysis of the mechanical strength of the structure

The biaxial modulus of elasticity of the studied structure was analyzed. Analyzing the dependence of the deflection

of the membrane  $w$  on the overpressure  $P$ , it is possible to determine the biaxial modulus of elasticity  $E/(1 - \mu)$  using the formula

$$\frac{E}{1 - \mu} = \frac{P \cdot a^4}{C_2 \cdot h \cdot w^3}, \quad (1)$$

where  $P$  is the overpressure,  $h$  is the membrane thickness,  $w$  is the membrane deflection,  $a$  is the membrane radius,  $E$  is the Young's modulus,  $\mu$  is the Poisson's ratio,  $C_2$  is the coefficient. Usually, when working with round membranes,  $C_2 = 8/3$  is used. The calculation of mechanical strength  $\sigma_{\max}$  is carried out according to the formula

$$\sigma_{\max} = \frac{3}{4} \cdot \frac{a^2 \cdot \sqrt{1 + \mu^2} \cdot P_{\text{cr}}}{h^2}, \quad (2)$$

where  $a$  is the membrane radius,  $h$  is the membrane thickness,  $P_{\text{cr}}$  is the critical membrane rupture pressure,  $\mu$  is the Poisson's ratio of the membrane.

#### 5. Study results

As a result of the analysis of the thin-film structure on AFM, it was found that the roughness of MoSiN grains varies from 1.5 to 3.0 nm (Figure 4). The method of analyzing SEM images of the surface was used to estimate the grain size using the ImageJ program (Figure 5). The calculation results are shown below for the initial MoSiN film (without additional heat treatment). The average grain size in the studied MoSiN structure was 22 nm (the grain size of MoSiN, measured using a transmission electron microscope, was 20 nm in [12]).

The critical overpressure of the membrane structures is  $0.05 \pm 0.003$  GPa for 10 samples. The experimental values of the modulus of elasticity and strength for the initial structure are 96 and 1.15 GPa, respectively. The article

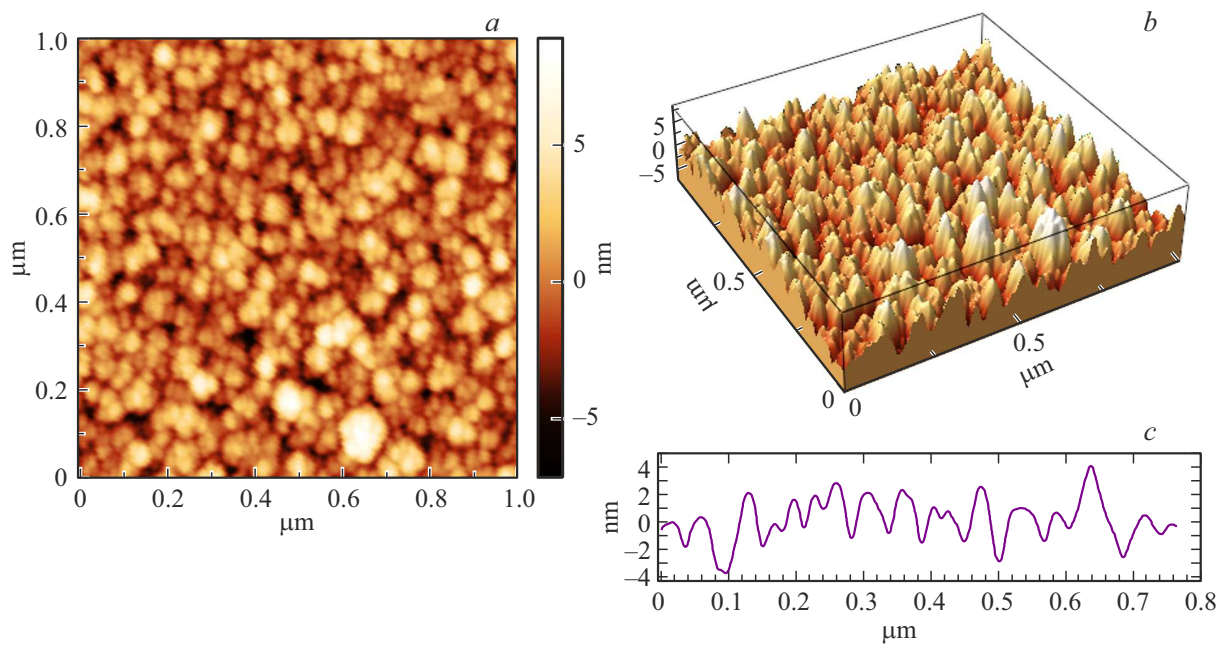


**Figure 4.** Analysis of the grain size of original MoSiN structure: *a* — AFM image, *b* — 3D AFM image, *c* — profile line.

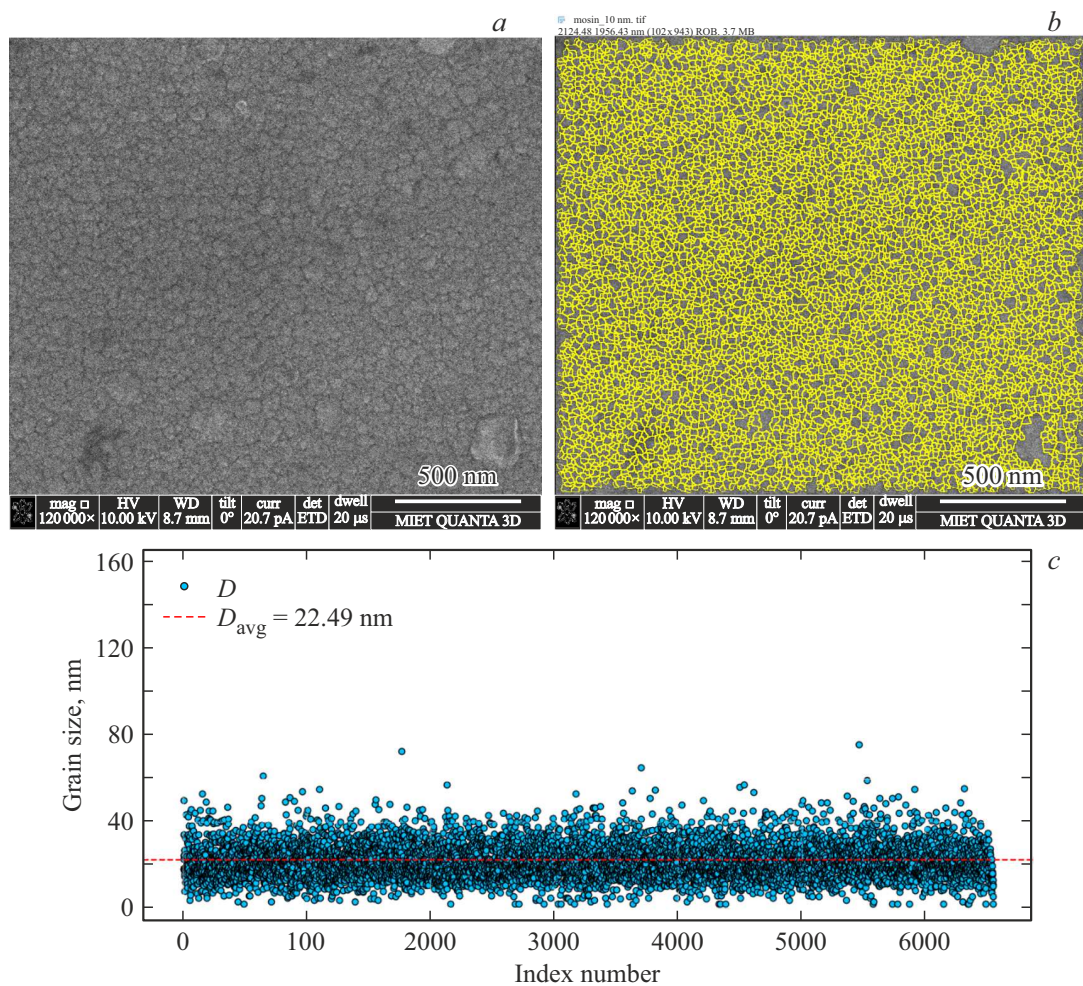


**Figure 5.** Analysis of the grain size of original MoSiN structure: *a* — SEM image, *b* — processed SEM image, *c* — grain size distribution depending on the conditional sequence number.

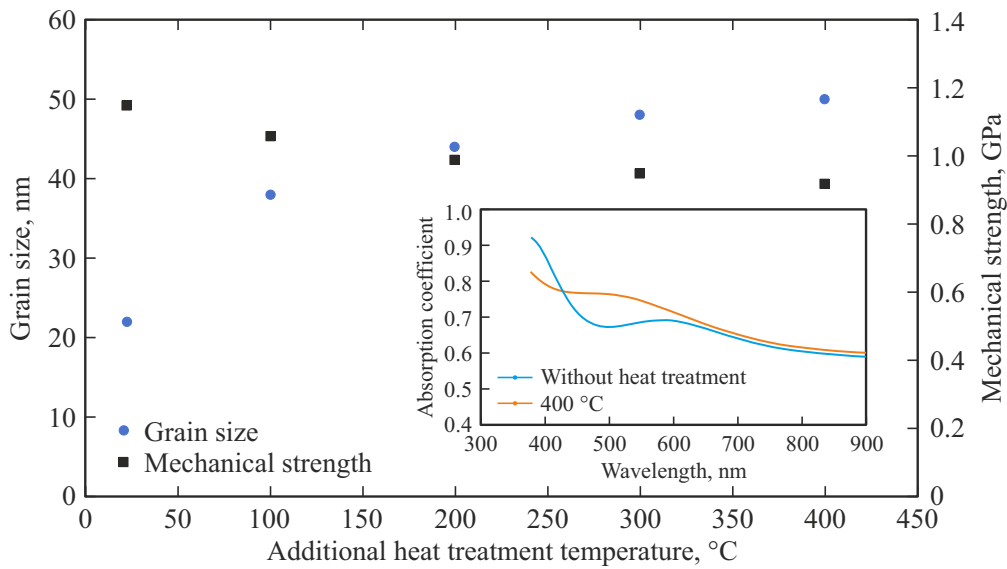


**Figure 6.** The effect of additional temperature treatment on structural, mechanical, and optical properties.

in Ref. [12] mentions that the Poisson's modulus, which is necessary for calculating the modulus of elasticity, for MoSiN is in the range 0.25–0.30.

Additional heat treatment of the initial MoSiN film was carried out at temperatures of 100, 200, 300 and 400 °C (Figure 6). With an increase in the heat treatment temperature [13,14], the grain size increases from 22 to 50 nm, the mechanical strength decreases from 1.15 to 0.92 GPa, and the absorption coefficient varies to a much lesser extent over the wavelength range from 400 to 900 nm.

It is known from Refs. [15,16] that the hardness of the MoSiN film is  $22 \pm 6$  GPa, Young's modulus varies from 214 to 253 GPa. The hardness of MoSiN varied in the range from 12.63 to 18.83 GPa in other studies [1,17], the Young's modulus ranged from 227 to 234 GPa. It is known [18] that the value of mechanical strength is 1/3 of the value of hardness. Thus, the results obtained correlate well with the results of other researchers' work.

## 6. Conclusion

It has been found that the grain size increases from 22 to 50 nm with an increase in the heat treatment temperature, the mechanical strength decreases from 1.15 to 0.92 GPa, and the absorption coefficient varies to a much lesser extent in the wavelength range from 400 to 900 nm. The roughness increases from 1.5 to 3.0 nm. The obtained result makes it possible to adjust the optical properties of the MoSiN coating material for specific wavelengths with a slight decrease in mechanical strength. A decrease in mechanical strength occurs due to an increase in grain size, which is consistent with the Hall–Petch ratio.

## Acknowledgments

The work was performed using MIET equipment within the framework of the state task in 2023–2025 under agreement FMSR-2023-0003.

## Conflict of interest

The authors declare no conflict of interest.

## References

- [1] J.J. Price, T. Xu, B. Zhang, L. Lin, K.W. Koch, E.L. Null, K.B. Reiman, C.A. Paulson, C.-G. Kim, S.-Y. Oh, D.-G. Moon, J.-H. Oh, A. Mayolet, C.K. Williams, S. D. Hart. *Coatings*, **11**, 213 (2021).
- [2] J.C. Caicedo, C. Amaya, L. Yate, M.E. Gómez, G. Zambrano, J. Alvarado-Rivera, J. Muñoz-Saldaña, P. Prieto. *Appl. Surf. Sci.*, **256** (20), 5898 (2010).
- [3] C. Jama, R. Delobel. *Multifunctional Barriers for Flexible Structure* (Heidelberg, Springer Berlin, 2007) v. 97, p. 109.
- [4] S. Chandramohan, A. Kanjilal, T. Strache, J.K. Tripathi, S.N. Sarangi, R. Sathyamoorthy, T. Som. *Appl. Surf. Sci.*, **256** (2), 465 (2009).
- [5] Z.-X. Lin, Y.-C. Liu, C.-R. Huang, M. Guillon, F.-B. Wu. *Surf. Coat. Technol.*, **383**, 125222 (2020).
- [6] Y. Choi, S. Suresh. *Acta Mater.*, **50**, 1881 (2002).
- [7] H. Choo, D. Seo, S. Lim. *Appl. Surf. Sci.*, **311**, 831 (2014).
- [8] S.-J. Yang, H.-S. Cha, J. Ahn, K.-S. Nam. *Proc. SPIE*, **7488**, 74880M (2009).
- [9] P. Torri, A. Mahiout, J. Koskinen, J.-P. Hirvonen, L.-S. Johansson. *Scr. Mater.*, **42** (6), 609 (2000).
- [10] M. Rothschild, R.B. Goodman, M.A. Hartney. *J. Vac. Sci. Technol. B*, **10**, 2989 (1992).
- [11] S.Yu. Zuev, A.Ya. Lopatin, V.I. Luchin, N.N. Salashchenko, D.A. Tatarsky, N.N. Tsybin, N.I. Chkhalo. *ZhTF* **89** (11), 1680 (2019). (in Russian).

- [12] Q. Liu, Q.F. Fang. *Surf. Coat. Technol.*, **201** (3–4), 1894 (2006).
- [13] M.V. Narykova, B.K. Kardashev, A.A. Levin, A.G. Kadomtsev, V.I. Betekhtin, A.I. Likhachev. *FTT*, **66** (6), 1008 (2024). (in Russian).
- [14] A.G. Kadomtsev, M.V. Narykova, V.I. Betekhtin, O.V. Amosova. *Phys. Solid State*, **65** (11), 1989 (2023). (in Russian).
- [15] C.-K. Jung, S.H. Jeong, Y.-M. Chung, J.-G. Han, J.-H. Boo. *Met. Mater. Int.*, **13**, 463 (2007).
- [16] Y.-C. Liu, B.-H. Liang, C.-R. Huang, F.-B. Wu. *Coatings*, **10**, 987 (2020).
- [17] B.-H. Liang, F.-S. Hsieh, F.-B. Wu. *Surf. Coat. Technol.*, **436**, 128278 (2022).
- [18] B. M. Clemens, H. Kung, S.A. Barnett. *MRS Bulletin*, **24** (2), 20 (1999).

*Translated by A.Akhtyamov*